Determination of Complex Permeability of Silicon Steel for Use in High-Frequency Modeling of Power Transformers

Article *in* IEEE Transactions on Magnetics · May 2008

DOI: 10.1109/TMAG.2007.914857 · Source: IEEE Xplore

4 authors, including:

Tadeusz Daszczyński
Warsaw University of Technology

Yuriy Serdyuk
Chalmers University of Technology

Stanislaw M. Gubanski
Chalmers University of Technology

Determination of Complex Permeability of Silicon Steel for Use in High-Frequency Modeling of Power Transformers

K. G. Nilanga B. Abeywickrama[1], Tadeusz Daszczyński[2], Yuriy V. Serdyuk[1], and Stanislaw M. Gubanski[1], *Fellow, IEEE*

[1]Division of High Voltage Engineering, Chalmers University of Technology, SE 412 96 Göteborg, Sweden
[2]Warsaw University of Technology, 00-611 Warsaw, Poland

Information about frequency dependence of complex permeability of silicon steel is a vital input parameter in calculations of transformer winding inductance used for modeling high-frequency behavior (100 Hz–1 MHz). We present two ways of determining small signal complex permeability spectra in frequency domain and compare and discuss the results. The first method is based on an optimization procedure, in which inductance of a winding is measured and calculated by analytical formulas and finite-element modeling. The second method makes use of a single sheet tester. We show that the magnitude of effective permeability of the silicon steel laminations remains significant up to about 100 kHz. We also report on the effect of magnetic viscosity on complex permeability.

Index Terms—**Complex permeability, magnetic viscosity, power transformers, silicon steel, single sheet tester.**

I. Introduction

SILICON steel, otherwise called electrical steel, is the most popular soft magnetic material in the electric power industry as the core material of electrical machines. Grain-oriented silicon steel is mainly used in manufacturing of transformer cores, which provides the required magnetic anisotropy and lowest losses when magnetized in the rolling direction [1]. Eddy-current losses are further reduced at power frequency (50/60 Hz) by using laminations of silicon steel. The laminations are normally insulated with a thin organic or inorganic surface coating for nonoriented silicon steel and by phosphate coating for grain-oriented silicon steel that prevents flow of inter-laminar currents. The laminations are typically produced in strips 0.35–0.8 mm thick for nonoriented grades and 0.23–0.35 mm thick for oriented grades [2].

Despite the fact that transformers work at power frequency, there are situations where the windings are exposed to high-frequency excitations, e.g., transient over voltages containing high-frequency components and during frequency response measurements. To analyze these phenomena in power transformers, high-frequency transformer models have been developed and lumped circuit modeling is one of the most frequently used approaches. In this approach, windings are split into finite sections that can be represented by lumped capacitances, conductances, inductances, and resistances. Permeability of the laminated core and its losses are the required input parameters for calculating inductance and effective resistance (including core losses and winding resistance) of the windings. However, at higher frequencies, the effective complex permeability of the core becomes frequency dependent due to repellence of magnetic flux out of the laminated core by the counteracting magnetic flux produced by increasing eddy currents.

The influence of the core has usually been neglected above 10 kHz [3] when modeling transformer windings for use in frequency response analysis (FRA). However, the authors have shown that the influence of the core remains significant even at frequencies above 100 kHz [4]. The purpose of the work described in this paper has therefore been twofold, i.e., 1) to estimate the small signal local permeability of silicon steel laminations indirectly by using an optimization procedure and thus obtaining the complex permeability spectra and 2) to experimentally determine the complex permeability spectra and the effect of magnetic viscosity on these spectra. In the study, a distribution type transformer (T1: 50 KVA, 11/0.4 kV, Yd11) was used for both the modeling and the measurements. A single sheet tester [5] based on impedance measurements (performed by means of an impedance analyzer HP4292A) was built for measuring the complex permeability of steel laminations taken out from the transformer. Samples of two other silicon steel grades originating from different manufacturers were also investigated.

II. Effective Complex Permeability of Silicon Steel Laminations

A. Complex Permeability

Magnetic induction and related phenomena inside a piece of steel lamination subjected to an external magnetic field can be derived from Maxwell's equations [6]. It is assumed in this derivation that displacement current density is negligible compared to the conduction current in the studied frequency range as well as the effect of electric field inside the insulation layer on the lamination. Fig. 1 shows a lamination sample of size $\triangle y \times \triangle z$ and thickness $2b$. $\triangle z$ is the length of the sample in the perpendicular direction to xy-plane. If eddy-current loops are assumed to be large enough along the y-direction, the field problem becomes one-dimensional and can be reduced to a single equation for z-component of the magnetic field $\hat{H}_z(x,t)$ that depends only on x:

$$\frac{\partial^2 \hat{H}_z(x,t)}{\partial x^2} = \mu_0 \mu_z \sigma \frac{\partial \hat{H}_z(x,t)}{\partial t}. \tag{1}$$

Digital Object Identifier 10.1109/TMAG.2007.914857

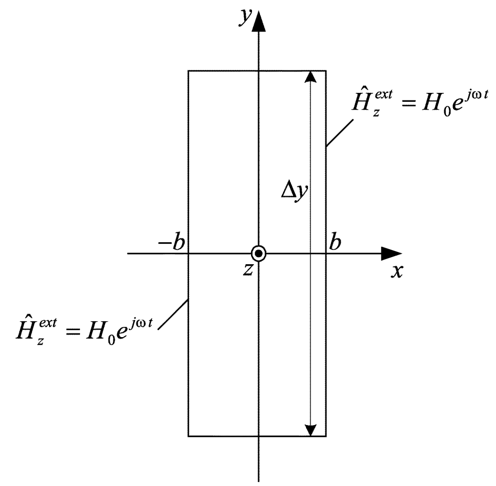

Fig. 1. Rectangular lamination sample placed on xy-plane.

For time-harmonic case (ω-angular frequency) with boundary condition $H_z(\pm b, t) = H_0 e^{j\omega t}$, solution of (1) can be represented as

$$H_z(x,t) = \frac{H_0}{1+e^{-2\gamma b}} \left(e^{j\omega t - \gamma(x+b)} + e^{j\omega t + \gamma(x+b)} \right). \quad (2)$$

Here, γ is the propagation constant defined as $\gamma = \sqrt{j\omega\mu_0\mu_z\sigma}$, which is directly related to the skin depth $\delta = \sqrt{2/\omega\mu_0\mu_z\sigma}$ by $\gamma = (1+j)/2\delta$. μ_z is the local relative permeability of the lamination sample in the z-direction and σ denotes the conductivity of silicon steel. Averaged magnetic flux density in z-direction $\langle \hat{B}_z \rangle$ can be evaluated in terms of total magnetic flux $\phi(t)$ through the cross section $(2b \cdot \Delta y)$ as

$$\langle \hat{B}_z \rangle = \frac{\phi(t)}{2b \cdot \Delta y} = \frac{\int_{-b}^{b} \mu_0 \mu_z H_z(x,t) \Delta y dx}{2b \cdot \Delta y} = H_0 e^{j\omega t} \frac{\mu_0 \mu_z}{\gamma} \tanh(\gamma b). \quad (3)$$

Thus, effective relative complex permeability in z-direction of a single lamination can be expressed as

$$\hat{\mu}_z^{eff} = \mu'_z - j\mu''_z = \frac{\langle \hat{B}_z \rangle}{\mu_0 \hat{H}_z^{\text{ext}}} = \mu_z \frac{\tanh(\gamma b)}{(\gamma b)}. \quad (4)$$

Similarly, the effective relative complex permeability in y-direction can be derived as

$$\hat{\mu}_y^{\text{eff}} = \mu'_y - j\mu''_y = \mu_y \frac{\tanh(\gamma b)}{(\gamma b)}. \quad (5)$$

Here, in calculating γ, μ_y should be used instead of μ_z. If we assume the following typical parameter values for 3% silicon steel: $\sigma = 5 \cdot 10^6$ S/m, $\mu_z = 500$, $\mu_y = \mu_z/2 = 250$, the resulting effective permeabilities as a functions of frequency are shown in Fig. 2.

B. Reluctance of a Fragment of Steel Lamination

Reluctance is a measure of the opposition to the magnetic flux driven by a magnetomotive force and it is analogous to the concept of resistance in an electric circuit. Reluctance is dependent on geometrical parameters as well as on permeability of the magnetic material. The magnetomotive force (MMF) that drives the amount of flux along the length Δz is $H_0 e^{j\omega t} \Delta z$. Division of MMF by the corresponding flux, as defined in (3), yields the reluctance $(\mathcal{R})$ of the lamination sample in z-direction as

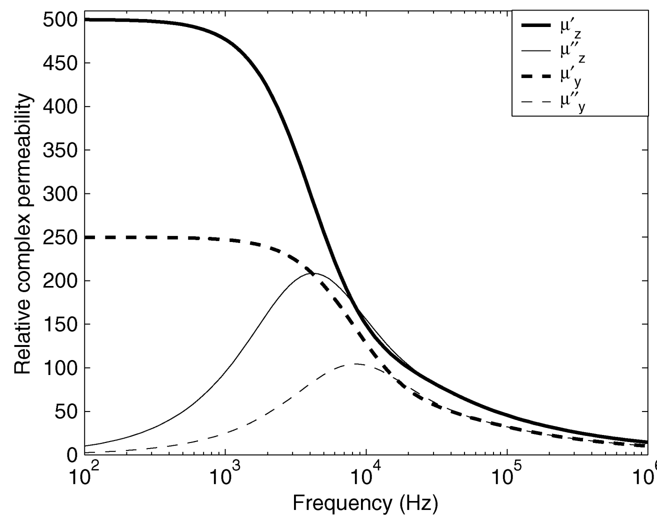

Fig. 2. Relative complex permeability of single lamination in z and y directions ($\hat{\mu}_z^{\text{eff}} = \mu'_z - j\mu''_z$ and $\hat{\mu}_y^{\text{eff}} = \mu'_y - j\mu''_y$) according to (4) and (5).

$$\mathcal{R} = \frac{\Delta z}{2b\mu_0 \hat{\mu}_z^{\text{eff}} \Delta y}. \quad (6)$$

This reluctance is a complex number that depends on frequency. If one can determine the frequency-dependent reluctance (6) of the lamination sample experimentally, the complex relative permeability can be calculated from

$$\hat{\mu}_z^{\text{eff}} = \frac{1}{\mu_0 \mathcal{R}} \cdot \frac{\Delta z}{2b\Delta y}. \quad (7)$$

III. Estimation of Small Signal Local Permeability (μ_z)

For calculating the effective permeabilities of both the bulk of the core [see (4)] and the mitered joint regions of a transformer core [4], the local permeability (μ_z) and conductivity (σ) of silicon steel are mandatory input parameters. These data are often unavailable, unless the manufacturers provide the information.

It is practically not possible to remove a lamination sample from a stacked core of a transformer for performing measurements of μ_z. Instead, one can estimate the small signal local permeability indirectly by using an optimization algorithm, in which inductance of a winding at a low frequency (<500 Hz) is numerically calculated and compared with a measured value. The reason for using this lower frequency inductance is to avoid the effect of winding capacitance, which together with the core inductance produces the first resonance of the measured impedance [7]. A flow diagram of the developed optimization algorithm is illustrated in Fig. 3. First, it makes use of realistically assumed initial values of the required parameters for calculating the winding inductance (calculation of permeability of the bulk lamination and the joints that is then used in a 3-D model of the transformer core to calculate the

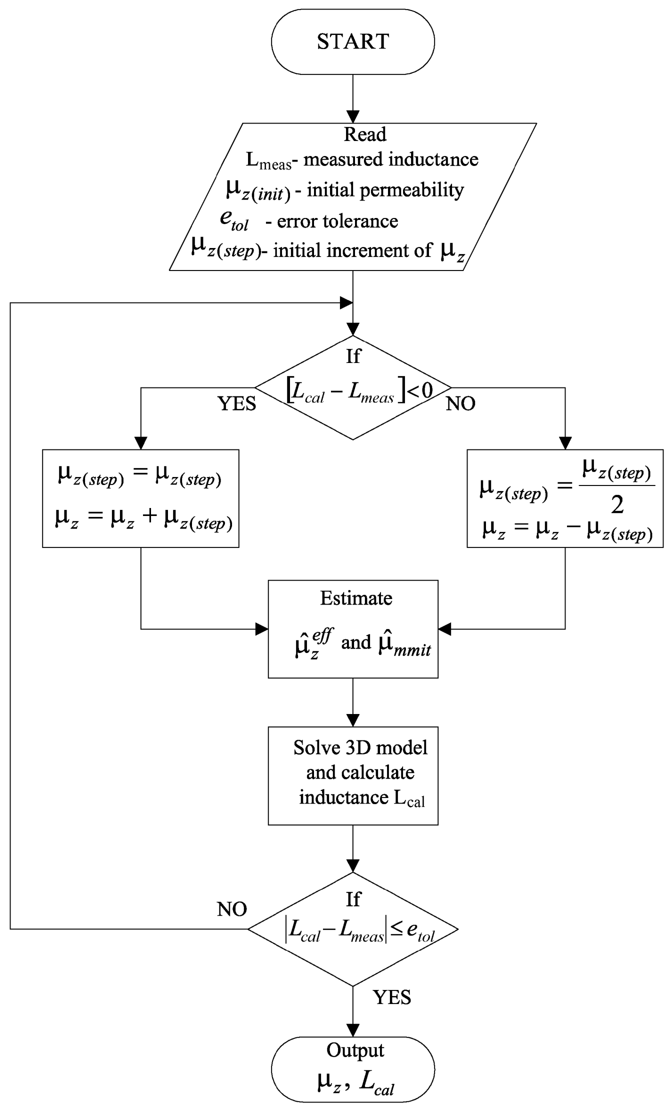

Fig. 3. Flowchart showing the basic steps of the algorithm used for estimating the small signal local permeability μ_z of electrical steel.

winding inductance) and then compares it with the measured one. Depending on the sign of the error in this comparison, an increment of μ_z is chosen and the calculation continues until the difference reaches a predefined error level. The iteration ends at this point and it yields the values of calculated inductance $L_{\rm cal}$ and μ_z.

Estimation of the complex permeabilities of bulk of the core ($\hat{\mu}_z^{\rm eff}$) and core joints ($\hat{\mu}_{mmit}$), and calculation of inductance of a winding (see Fig. 3) were performed by means of 2-D and 3-D finite-element models developed by the authors [4], [8], [9]. The whole algorithm was implemented as a script in a finite element software COMSOL Multiphysics [10].

The optimization procedure was applied to transformer T1. The measured inductance value ($L_{\rm meas}$) of T1 was 25 mH at 500 Hz. The algorithm started with initial conditions $\mu_{z({\rm init})} = 400$, $\mu_{z({\rm step})} = 100$ and error tolerance $e_{\rm tol} = L_{\rm meas}/10^3$, and after 10 iterations it estimated that the local permeability in the z-direction is 448, which appeared a bit higher than the measured value (438).

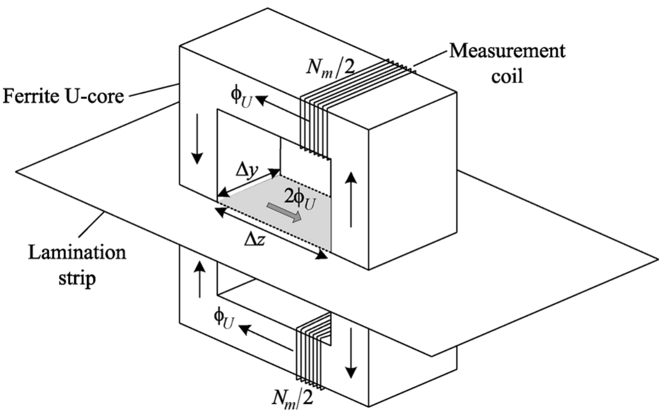

Fig. 4. Single sheet tester.

IV. Complex Permeability Measurements

If a lamination sample is available, there is always a possibility to measure complex relative permeability. Not only μ_z at a single frequency, but also measurements of the frequency response of the complex permeability in a desired direction with respect to the rolling direction are possible. Properties of silicon steel are usually determined by means of Epstein frame method or single sheet tester as recommended by IEC-Standards (IEC 404-2 [11] and IEC 404-3 [12]). These types of measurements focus on specific power loss (W/kg) and permeability at power frequency (50 or 60 Hz). For the purpose of this paper Epstein frame method is not suitable, as it determines properties of a stack of lamination with joints. Although the single sheet tester is ideal for measuring characteristics of a single sheet of silicon steel at power frequency, the double yoke system made up of grain-oriented silicon steel or nickel iron alloy, as recommended by IEC 404-3 to provide low reluctance path, makes it unsuitable for determining the high-frequency characteristics of the test specimen. Therefore, a high-permeability material with sufficiently flat high-frequency characteristics (permeability and losses) should be used instead for the yokes.

A. Single Sheet Tester

Measurements of complex permeability were carried out using the single sheet tester (see Fig. 4) proposed by Roger *et al.* [5]. The tested lamination strip is placed in between two U-type high permeability ferrite cores (MAGNETICS Ferrites, $\mu \approx 2500$, 50% roll-off frequency 1.2 MHz [13]) as shown in Fig. 4. This arrangement provides very low reluctance for the rest of the magnetic path around the test specimen. Size of the lamination strip (30×30 cm^2) was selected so that the large enhancement of the magnetic field at the edges of the strip does not affect the tested area between yokes. The tested area (shaded region in Fig. 4, 2.5×5 cm^2) should also be sufficiently large in order to avoid the possible influence of material heterogeneity [14]. A clamping structure was made up of plexiglass in order to hold two yokes tightly against the test sample, leaving no air gaps between the sample surface and the yoke face. This is a very important issue when calculating the reluctance of the test specimen due to the fact that even a small air gap could result in a significant error in the measurements [15]. Two measuring coils (20 turns each connected in series) were wound on each

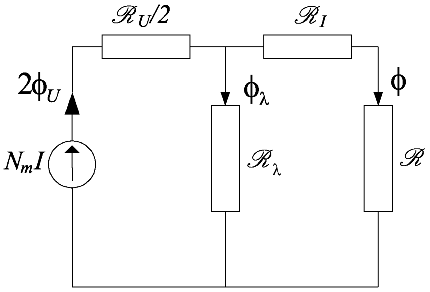

Fig. 5. Equivalent magnetic circuit of single sheet tester in Fig. 4.

on the U-core (see Fig. 4) and their impedance at different frequencies (100 Hz–1 MHz) was recorded by the impedance analyzer.

B. Interpretation of Measurements

The equivalent magnetic circuit of the experimental setup (Fig. 4) is depicted in Fig. 5. Two coils connected in series produce the same amount of flux. In Fig. 5, $\mathcal{R}_U$ is the reluctance of the ferrite yoke, $\mathcal{R}_I$ represents the reluctance of the gap between the yokes and the lamination strip, which appears due to the insulation layer on the lamination strip. $\mathcal{R}_\lambda$ stands for the leakage reluctance accounting for leakage flux outside lamination strip and $\mathcal{R}$ is the reluctance of the tested area of the lamination strip. Flux density in the yokes during the measurements was kept very small so that $\mathcal{R}_U$ remained constant. The other two reluctance values ($\mathcal{R}_I$ and $\mathcal{R}_\lambda$) were also not dependent on the flux density [5].

Equivalent permeance of the whole magnetic circuit (Fig. 5) can be simplified by placing $\mathcal{R}_\lambda$ before $\mathcal{R}_U/2$ and expressed as

$$\mathcal{P}_{eq} = \frac{1}{\mathcal{R}_\lambda} + \frac{1}{\mathcal{R} + \mathcal{R}_I + \mathcal{R}_U/2} \tag{8}$$

thus, the reluctance of the lamination sample becomes

$$\mathcal{R} = \frac{1}{\mathcal{P}_{eq} - \mathcal{P}_\lambda} - \left(\frac{1}{\mathcal{P}_I} + \frac{1}{2\mathcal{P}_U}\right). \tag{9}$$

Knowing the permeance of a magnetic circuit, number of turns of the coil (N_m) and neglecting the copper wire resistance, the inductance of the measuring coil can be expressed as $N_m^2\mathcal{P}$ [16]. Hence, the impedance of the two series-connected coils is given by

$$Z = j\omega N_m^2 \mathcal{P}. \tag{10}$$

Therefore, corresponding permeance values can be determined by the following measurements.

- Impedance measurement with the lamination strip provides the equivalent impedance (Z_{eq}) of the test setup. Then, it is possible to calculate $\mathcal{P}_{eq}$ from $Z_{eq} = j\omega N_m^2 \mathcal{P}_{eq}$, which is frequency dependent.
- Impedance measurement without lamination strip provides the leakage impedance (Z_λ) of the test setup, as the equal and oppositely directed magnetic flux in the yokes cancel each other and only the leakage flux remains. Thus, $\mathcal{P}_\lambda$ can be calculated from $Z_\lambda = j\omega N_m^2 \mathcal{P}_\lambda$, $(\mathcal{P}_\lambda = 0.1435\ \mu\text{H})$.

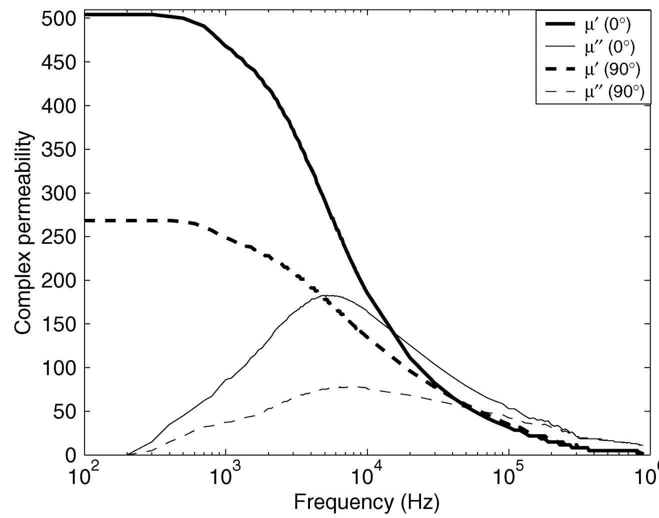

Fig. 6. Measured relative complex permeability of lamination sample 30H102 in the rolling direction and transverse direction.

- Impedance measurement without lamination strip and two coils connected in series with opposite directions compared with previous measurement force the flux into the ferrite yokes. Hence, the permeance of yokes $\mathcal{P}_U$ can be calculated from $Z_U = j\omega N_m^2 \mathcal{P}_U$, $(\mathcal{P}_U = 10.755\ \mu\text{H})$.
- Permeance of small insulation gap $(\mathcal{P}_I)$ is approximately calculated using geometrical parameters $(\mathcal{P}_I \approx 20\ \mu\text{H})$.

When $\mathcal{P}_\lambda$, $\mathcal{P}_I$, $\mathcal{P}_U$, and $\mathcal{P}_{eq}$ are known, one can calculate the complex reluctance of the lamination sample $\mathcal{R}$. Then, the relative complex permeability can be calculated by means of (7). Here, the length of the magnetic path (Δz) in the test sample is defined as the inner distance between the yoke faces as shown in Fig. 4 as recommended in [12]. One should notice here that the dc and ac resistances of the wire are also included in all the impedance measurements. These are calculated analytically and deducted from the measured impedance (10).

Relative complex permeabilities of lamination strips taken out from T1 and of two other silicon steel samples (30H102 and 30R122) were determined by means of the aforementioned procedure. Figs. 6–8 illustrate the obtained results. Two samples of 30H102 and 30R122 steel exhibit different local permeability (μ_z) values in the rolling direction; 504 for 30H102 and 472 for 30R122. Consequently, the loss peak appears at lower frequency for 30H102 (5.46 kHz) compared to 30R122 (6.9 kHz) (the higher the local permeability the lower the frequency of the loss peak). The complex permeability in the transverse direction showed anisotropy factor $\mu_z/\mu_y \approx 1.8$, which could be explained by crystallographic anisotropy of silicon steel [17], [18]. The lamination sample taken out from T1, which is a very old transformer, exhibited lower local permeability (438) compared to new samples.

It can clearly be noticed from Figs. 6–8 that at 10 kHz, above which the influence of the magnetic core is often neglected in modeling transformers for FRA purposes, the permeability falls down to ~45% of its low-frequency value. Therefore, the negligence of the core influence above 10 kHz is not justified at

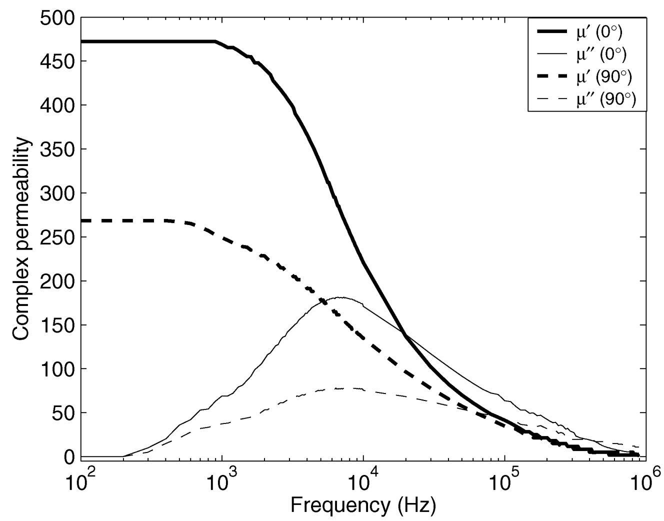

Fig. 7. Measured relative complex permeability of lamination sample 30R122 in the rolling direction and transverse direction.

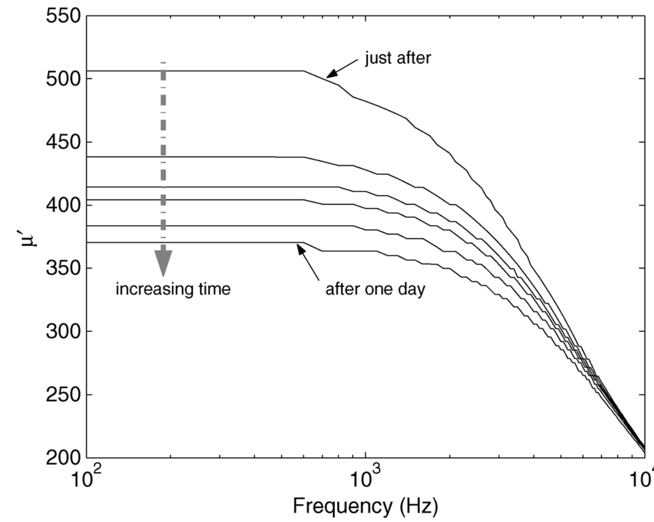

Fig. 9. Change in real part of the complex permeability with time after sudden removal of dc magnetization from a steel sample of T1.

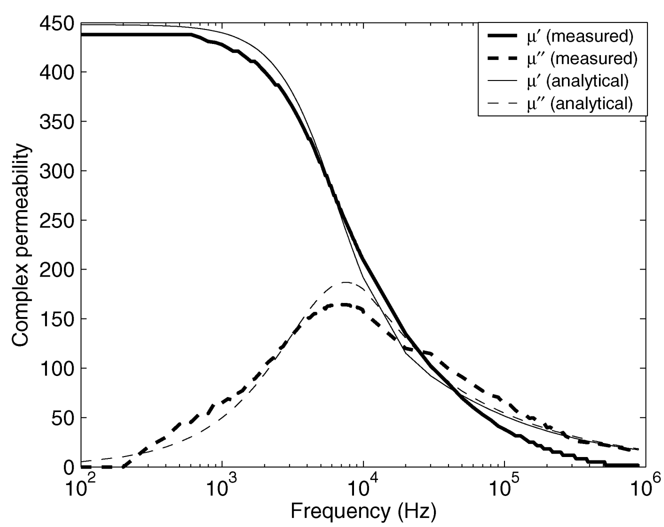

Fig. 8. Measured and analytically calculated relative complex permeability of lamination sample of T1 in the rolling direction.

all, as the silicon steel further supports magnetic flux well up to ~100 kHz ($\mu'_{100\ \mathrm{kHz}}/\mu_z \times 100 \approx 8.5\%$).

The measurements of complex permeability provide a possibility to evaluate actual conductivity of steel by applying optimization algorithm that minimizes the error between the measured and calculated [using (5)] permeability spectra, where σ is treated as unknown parameter [5]. Such an algorithm was implemented in Matlab and is based on least-square nonlinear curve fitting technique with 200 frequency points ranging from 100 Hz to 1 MHz. The procedure was applied to data obtained for a steel sample taken from transformer T1 and its conductivity was found to be $4 \times 10^6\ \mathrm{Sm}^{-1}$. This value was further used for calculating permeability spectra and the results are shown in Fig. 8. The calculated complex permeability spectra were obtained by means of (5) with parameters $\mu_z = 448$ (estimated in Section III). One can observe that, at low frequencies, the measured real part of the permeability appears lower because the estimated μ_z (448) is higher than the measured one (438). The measured real part also becomes lower compared with the analytical prediction at higher frequencies. This could result from the fact that the analytical expression used is derived by considering only the classical eddy-current approach.

V. Effect of Magnetic Viscosity on Complex Permeability Spectra

It was found in authors' previous study [19] that the low-frequency response of winding impedance is affected by magnetic viscosity, yielding relaxation in permeability over a long period of time. To investigate this phenomenon, another lamination sample was taken out from the core of the transformer T1 and tested as described in the previous section. An additional coil was wound on the steel sample and supplied with a dc current so that the amount of MMF produced by the coil was enough to drive the lamination sample into saturation. Then, the dc current was suddenly removed and the measurements were conducted over a one-day period. Figs. 9 and 10 depict the time varying real and imaginary parts of the relative complex permeability in the rolling direction. The real part jumped to a higher value and started relaxing towards a steady state. Fig. 11 shows the impedance spectrum of the low voltage winding on an outer limb of transformer T1, which was measured after sudden removal of the dc magnetization from the core [19]. One can readily see the analogy between the variations of the real part of the permeability (Fig. 9) and changes in measured impedance. The imaginary part of the permeability, which is directly related to losses in the steel laminations, is also decreasing with time and its peak is shifting towards higher frequencies (due to decreasing μ_z [4]). If one takes a closer look at the variation of the first peak of impedance, the increase in magnitude of the peak (less damping) with time (see Fig. 11) is a direct consequence of the decreasing imaginary part of the permeability (Fig. 10).

It is known that the characteristics of viscosity can be described using a logarithmic function [20], [21]. Fig. 12 shows the decay of permeability at 800 Hz fitted with a function in the form of $\mu(t) = \mu(0) - S_\mu \cdot ln(t/t_0)$. It is seen that the logarithmic function can well approximate only the initial part

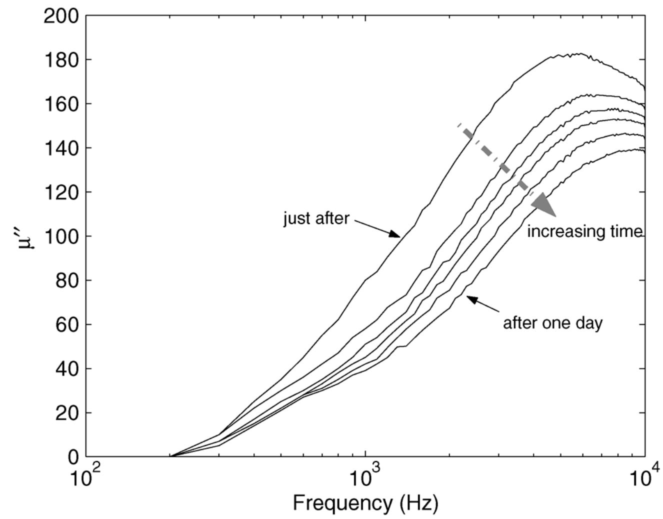

Fig. 10. Change in imaginary part of the complex permeability with time after sudden removal of dc magnetization from a steel sample of T1.

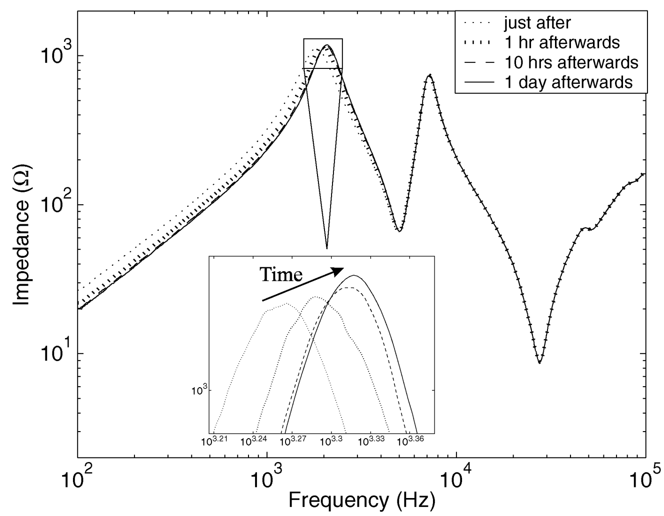

Fig. 11. Variation of impedance (LV winding on an outer limb) with time after sudden removal of dc magnetization to the core of T1.

of the viscosity effect. However, it cannot be used to describe permeability change when approaching the steady-state value at $t \longrightarrow \infty$. Moreover, it is not possible to evaluate single effective relaxation time from Fig. 12 due to complex and distributed nature of relaxation processes [21], [22].

VI. Conclusion

Anisotropic complex permeability spectra (in the frequency range 100 Hz–1 MHz) of silicon steel laminations, used for power transformers, have been measured by means of a single sheet tester. Furthermore, it has been used to investigate the viscous nature of the permeability after sudden removal of magnetization. An optimization algorithm has also been developed to determine the complex permeability when no steel sample is available for measurements.

It was found from the measurements performed by the single sheet tester that silicon steel laminations can support magnetic flux well up to ~100 kHz. Therefore, the influence of ferromagnetic core cannot be neglected above 10 kHz in

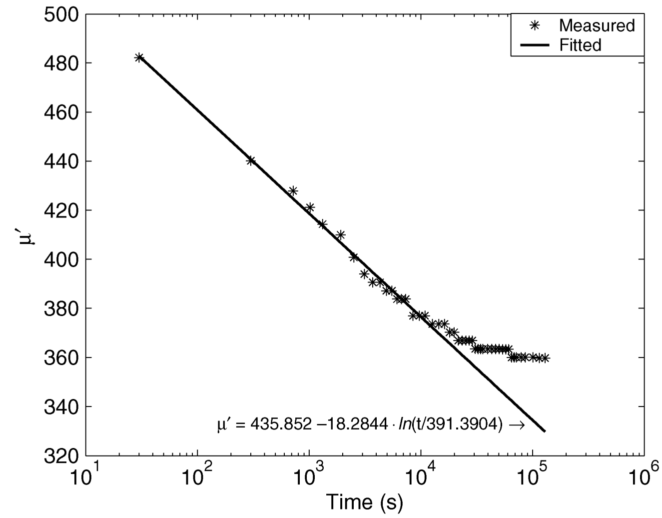

Fig. 12. Change in imaginary part of the complex permeability at 800 Hz with time after sudden removal of dc magnetization. Solid lines represent fitted logarithmic approximation.

high-frequency modeling of power transformers. Magnetic viscosity measurements confirm that the frequency response measurements (<10 kHz) on transformers can be affected by viscous nature of complex permeability. This effect may extend in time for about one day (see Fig. 12) after a change in magnetization.

Acknowledgment

This work was supported by SIDA-SAREC of Sweden and ABB/SECRC.

References

[1] S. Tumanski, "Investigation of the anisotropic behaviour of SiFe steel," *J. Magn. Magn. Mater.*, vol. 254, pp. 50–53, 2003.

[2] A. J. Moses, "Electrical steels: Past, present and future developments," *Inst. Elect. Eng. Proc.*, vol. 37, no. 5, pp. 223–245, Sep. 1990.

[3] E. Rahimpour, J. Christian, K. Feser, and H. Mohseni, "Transfer function method to diagnose axial displacement and radial deformation of transformer windings," *IEEE Trans. Power Del.*, vol. 18, no. 2, pp. 493–505, Apr. 2003.

[4] K. G. N. B. Abeywickrama, A. D. Podoltsev, Y. V. Serdyuk, and S. M. Gubanski, "Computation of parameters of power transformer windings for use in frequency response analysis," *IEEE Trans. Magn.*, vol. 43, no. 5, pp. 1983–1990, May 2007.

[5] D. Roger, E. Napieralska-Juszczak, and A. Henneton, "High frequency extension of non-linear models of laminated cores," *Int. J. Comput. Math. Elect. Electron. Eng.*, vol. 25, no. 1, pp. 140–156, 2006.

[6] J. Lammeraner and M. Stafl, *Eddy Current*. London, U.K.: ILIFFE Books, 1966.

[7] K. G. N. B. Abeywickrama, Y. V. Serdyuk, and S. M. Gubanski, "Exploring possibilities for characterization of power transformer insulation by frequency response analysis (FRA)," *IEEE Trans. Power Del.*, vol. 21, no. 3, pp. 1375–1382, Jul. 2006.

[8] A. D. Podoltsev, K. G. N. B. Abeywickrama, Y. V. Serdyuk, and S. M. Gubanski, "Multi-scale computations of parameters of power transformer windings at high frequencies. Part I: Small-scale level," *IEEE Trans. Magn.*, vol. 43, no. 11, pp. 3991–3998, Nov. 2007.

[9] A. D. Podoltsev, K. G. N. B. Abeywickrama, Y. V. Serdyuk, and S. M. Gubanski, "Multi-scale computations of parameters of power transformer windings at high frequencies. Part II: Large-scale level," *IEEE Trans. Magn.*, vol. 43, no. 12, pp. 4076–4082, Dec. 2007.

[10] COMSOL Multiphysics 3.2, Comsol AB. Stockholm, Sweden [Online]. Available: www.comsol.com

[11] *Magnetic Materials Part-2: Method of Measurements of the Magnetic Properties of Electrical Steel Sheet and Strip by Means of An Enstein Frame*, IEC Standard 60404-2, 1996.

[12] *Magnetic Materials Part-3: Method of Measurements of the Magnetic Properties of Electrical Steel Sheet and Strip by Means of a Single Sheet Tester*, IEC Standard 60404-3, 1992.

[13] MAGNETICS Ferrite Core Material Catalog [Online]. Available: http://www.mag-inc.com/pdf/2006_Ferrite_Catalog/2006_Materials.pdf

[14] S. Tumanski and T. Bakon, "Measuring system for two-dimensional testing of electrical steel," *J. Magn. Magn. Mater.*, vol. 25, no. 1, pp. 315–352, 2001.

[15] O. Stupakov, I. Tomàš, and J. Kadlecovà, "Optimization of single-yoke magnetic testing by surface fields measurement," *J. Phys. D: Appl. Phys.*, vol. 39, pp. 248–254, Jan. 2006.

[16] L. Dixon, "Deriving the equivalent electrical circuit from the magnetic device physical properties," Texas Instruments, 2003 [Online]. Available: http://focus.ti.com/lit/ml/slup198/slup198.pdf

[17] H. J. Williams, "Magnetic properties of single crystals of silicon iron," *Phys. Rev.*, vol. 52, pp. 747–751, Oct. 1937.

[18] V. D. Solovei and Y. N. Dragoshanskii, "Magnetic anisotropy constants of a Fe-3.8% Si single crystal," *Phys. Met. Metallogr.*, vol. 103, no. 1, pp. 33–38, 2007.

[19] K. G. N. B. Abeywickrama, Y. V. Serdyuk, and S. M. Gubanski, "Effect of core magnetization on frequency response analysis of power transformers (FRA)," *IEEE Trans. Power Del.*, accepted for publication.

[20] G. Bertotti, *Hysteresis in Magnetism*. San Diego, CA: Academic, 1998.

[21] D. C. Crew, P. G. McCormik, and R. Street, "The interpretation of magnetic viscosity," *J. Phys. D: Appl. Phys.*, vol. 29, no. 9, pp. 2313–2319, 1996.

[22] A. Lyberatos and R. W. Chantrell, "Fluctuation field of ferromagnetic materials," *J. Phys.: Condens. Matter*, vol. 9, no. 12, pp. 2623–2643, Apr. 1997.

Manuscript received August 17, 2007; revised December 14, 2007. Corresponding author: K. G. N. B. Abeywickrama (e-mail: nilanga.abeywickrama@chalmers.se).

K. G. Nilanga B. Abeywickrama (S'04) received the B.Sc. degree in electrical and electronic engineering in 2001 and the M.Sc. degree in electrical power and energy in 2003 from the University of Peradeniya, Sri Lanka, and the Lic. Eng. degree in 2005 from Chalmers University of Technology (CTH), Göteborg, Sweden, where he is currently pursuing the Ph.D. degree. His research interests include high-frequency modeling, high-frequency measurements, and diagnosis of power transformers.

Tadeusz Daszczyński received the M.Sc. degree in electrical engineering from the Warsaw University of Technology, Warsaw, Poland, in 2007. He was a visiting student at Chalmers University of Technology (CTH), Göteborg, Sweden, during academic year 2006–07, where he wrote his master thesis on high-frequency properties of silicon steel laminations.

Yuriy V. Serdyuk received the M.Sc. and Ph.D. degrees in high-voltage engineering from the National Technical University of Ukraine "Kiev Polytechnic Institute" Kiev, Ukraine, in 1986 and 1995, respectively.

From 1986, he worked as an engineer, and since 1991, as a researcher at the institute of Electrodynamics of the National Academy of Science of Ukraine Kiev. In 1996–1997, he was a Research Engineer at the R & D HV Laboratory, ABB High Voltage Technologies Ltd, Zurich, Switzerland. Currently, he is an Associate Professor in High Voltage Engineering, Department of Manufacturing and Materials Technology, Chalmers University of Technology, Göteborg, Sweden.

Stanislaw M. Gubanski (M'89–SM'90–F'01) received the M.Sc. degree in high-voltage engineering and the Ph.D. degree in material science from the Technical University of Wroclaw, Poland, in 1973 and 1976, respectively.

He was a Research Fellow at the University College of North Wales, Bangor, U.K., from 1976 to 1977, and a Senior Lecturer at the Technical University of Wroclaw, Wroclaw, Poland, from 1977 to 1988. Afterwards, he was Associate Professor at the Royal Institute of Technology, Stockholm, Sweden. Currently, he is Professor in High Voltage Engineering at the Department of Materials and Manufacturing Technology, Chalmers University of Technology, Göteborg, Sweden, and research leader of High Voltage Valley in Ludvika, Sweden. He is Chair of the IEEE-DEIS Nominations Committee. He is also convener of the CIGRE Task Force D1.01.14 "Dielectric Response Methods for Diagnostics of Power Transformers."